

Rapid Prototyping of Parafilm®-based analytical microfluidic devices using laser ablation and thermal fusion bonding

Yuanyuan Wei

The Chinese University of Hong Kong

Tianle Wang

The Chinese University of Hong Kong

Yuye Wang

Chinese Academy of Science

Yi-Ping Ho

The Chinese University of Hong Kong

Ho-Pui Ho (✉ aaron.ho@cuhk.edu.hk)

The Chinese University of Hong Kong

Article

Keywords: Microfluidics, Laser ablation, Thermal bonding

Posted Date: April 22nd, 2022

DOI: <https://doi.org/10.21203/rs.3.rs-1564490/v1>

License:  This work is licensed under a Creative Commons Attribution 4.0 International License.

[Read Full License](#)

Rapid Prototyping of Parafilm[®]-based analytical microfluidic devices using laser ablation and thermal fusion bonding

Yuanyuan Wei¹, Tianle Wang¹, Yuye Wang², Yi-Ping Ho^{1,3,4,5,*}, Ho-Pui Ho^{1,*}

¹Department of Biomedical Engineering, The Chinese University of Hong Kong, Shatin, Hong Kong, China. E-mail: ypho@cuhk.edu.hk; aaron.ho@cuhk.edu.hk

²Laboratory of Biomedical Microsystems and Nano Devices, Bionic Sensing and Intelligence Center, Institute of Biomedical and Health Engineering, Shenzhen Institutes of Advanced Technology, Chinese Academy of Science, Shenzhen 518055, China

³Centre for Biomaterials, The Chinese University of Hong Kong, Hong Kong SAR, China

⁴Hong Kong Branch of CAS Center for Excellence in Animal Evolution and Genetics, Hong Kong SAR, China

⁵The Ministry of Education Key Laboratory of Regeneration Medicine, Hong Kong SAR, China

Abstract

Parafilm[®] is a thermoplastic film extensively used in laboratories for sealing or protecting flasks or cuvettes. In this paper, we report a simple, low-cost, biocompatible and detachable microfluidic chip incorporating easily accessible polymethylmethacrylate (PMMA), PVC and glass slides as the substrate materials, along with Parafilm[®] as the bonding material. Multi-layer microfluidic chips can be fabricated by laser ablation followed by thermal fusion of constituent layers. A CO₂ laser ablation method was employed to cut substrates as well as the Parafilm[®] to obtain desired patterns. A thermal fusion bonding method was developed to bond the substrates in a single step. The patterned Parafilm[®] was sandwiched in the PMMA, PVC or glass layers, and heating of the assembly with the addition of a static pressure, various functional microfluidic elements including microvalves, micropumps, and bioreactors were demonstrated. With Parafilm[®] serving as a flexible membrane integrated to a fluidic channel, it was possible to implement a microvalve. A peristaltic micropump consisting of a sequence of interconnected gas-actuated microvalves was also fabricated. In addition, the biocompatibility of the PLT (Parafilm[®] based laser ablation and thermal fusion bonding fabrication method) fabricated bioreactor was validated by culturing GFP-expressing *E. coli*, results showed bacterium were able maintain growth in a 7-day post-cultivation. In summary, the reported fabrication scheme, offers an inexpensive and versatile alternative for rapid prototyping of common microfluidic devices.

Keywords: Microfluidics, Laser ablation, Thermal bonding

Introduction

Microfluidics is a rapidly growing research discipline due to its highly attractive features including device miniaturization, hence drastic reduction in reagent consumption, portability, low-cost, ease of volume production and compatibility with conventional integrated circuit manufacturing processes. Microfluidic devices have found application in chemical analysis, processing and analysis of biological samples, and disease diagnostics.^{1,2} A common fabrication process of microfluidic devices is soft-lithography utilizing flexible polymers such as polydimethylsiloxane (PDMS) to imprint and transfer patterned structures from

a mold.^{3,4} To this end, PDMS, a silicone-based elastomer, plays an important role in microfluidics because of its properties such as low surface interfacial free energy, optical transparency, gas permeability, and large elasticity, which are desirable characteristics for practical application where the microfluidic system is required to offer built-in micropumps, microvalves and the possibility of in situ optical excitation and detection.⁵⁻⁷

Despite the above mentioned merits, recent studies have revealed some significant drawbacks of PDMS, such as adsorption of hydrophobic molecules, short-term stability after surface treatment (such as hydrophilic stability after Oxygen plasma treatment), swelling in organic solvents, water permeability, and incompatibility with very high pressure operations.^{8,9} In addition, PDMS is incompatible with large-scale microfluidic device manufacture and packaging.² The fabrication of PDMS replicas is still a multistep process requiring photolithography using a photomask and the manufacture of mold. Consequently, PDMS may not be the ideal process of choice for fast prototyping for microfluidic devices. Another disadvantage of PDMS is the difficulty of building complex 3D structures by stacking multiple layers together, as bonding of PDMS typically requires a silane coupling agent to treat the PDMS surface, and device construction is done by bonding one layer at a time in a sequential manner. Despite the fact that conventional soft lithography may easily achieve fine structures, the method is often considered as costly and time-consuming due to the necessity for a cleanroom environment and expensive facilities.¹⁰

Recent research efforts have been attempting to discover alternatives to the conventional cleanroom-based soft lithography method, motivated by the growing demand for inexpensive and adaptable microfluidic chips and lab-on-a-chip (LOC) systems. One such endeavor entails replacing costly ultraviolet (UV) exposure machines with comparatively low-cost light sources such as sunshine,¹¹ or a confocal microscope's laser source. Other researchers looked at the problem from the standpoint of material selection to replace PDMS with ordinary printing paper¹² or thermal plastics¹³ for the substrate, and the use of functional films¹³ or wax^{12,14} as the bonding medium. Among these efforts, paper-based substrates possess several fundamental limitations, which include reaction with liquid molecules via absorption, have prevented their prospect as PDMS substitute. In addition, while hot-melt adhesive wax has been shown to be useful as a bonding material for various substrates (e.g. paper, PMMA, glass, and metal) with good sealing performance in 15-day long cell culture experiments,¹⁴ patterning and thickness uniformity issues are still challenging.

Besides, attention is shifted towards laser ablation technique, which have been shown to offer high versatility and cost-effectiveness for the manufacture of microfluidic devices. Several other studies have reported laser-plotted replica-molds for PDMS-based microchannels and thermal plastic microfluidic chips.¹⁵⁻¹⁷ Thermoplastics have inherent mechanical deformation resistance and chemical resistance. As a result, they've sparked a lot of interest as a viable alternative to traditional materials like PDMS, especially for commercial product-oriented applications. Parafilm[®], as a thermoplastic material (softening begins at approximately 60 °C) and a very common laboratory item, has also been employed in rapid prototyping as a low-temperature bonding material.¹⁸⁻²⁰

In this paper, we report a rapid and low-cost prototyping method for the fabrication of Parafilm[®]-based analytical microfluidic devices using laser ablation and thermal fusion bonding method (PLT). A schematic of the technique is shown in Fig.1. Laser ablation as well as one-step bonding of multiple layers to form a 3D structure can be realized without the necessity of photolithography and prefabricated master molds for pattern transfer. Firstly, the fabrication parameters of laser ablation and thermal fusion bonding process have been optimized respectively. Secondly, variation of bonding strength across different substrates and incubation conditions has also been characterized. The mechanical properties of Parafilm[®]-based elastomer have been studied. Practical actuation devices fabricated using this PLT method which include microvalves

and micropumps, have been demonstrated. In addition, biocompatibility of the PLT fabricated bioreactor has been investigated. Finally, a comparison between PLT approach and other fabrication techniques in terms of major application attributes are summarized. The reported PLT fabrication approach offers an economical and practical alternative for the rapid prototyping of for robust and complex microfluidic chips.

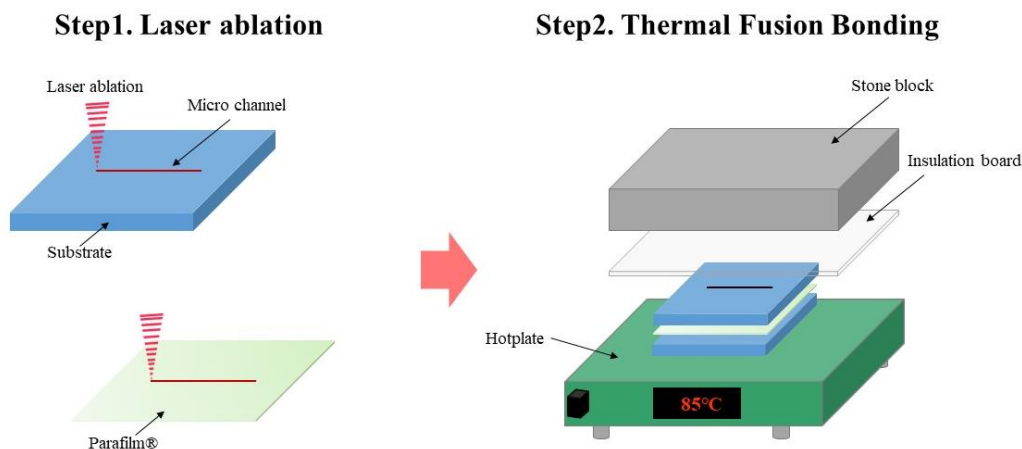


Fig. 1. Fabrication process flow of the Parafilm® based laser ablation and thermal fusion bonding (PLT) fabrication method. One Parafilm® film been cut to desired dimensions was aligned and sandwiched between two PMMA substrates. The assembly was placed on a hotplate with insulation board and stone block at the top for uniform static pressure and constant heating.

Methods

Laser ablation

Raw-cast transparent PMMA sheets in various thicknesses (1 - 5 mm) and Parafilm® M (Pechiney Plastic Packaging Company) were used in our experiments. All laser-cutting procedures were performed using a commercial CO₂ laser system (Maximum power: 80W, focal spot size: ~ 0.2 mm, Model CMA960, GD Han's Yueming Laser Group Co., Ltd.) as is shown in Supplementary Figure S1. All chip designs were implemented using Solidworks2016 and AutoCAD2018, which were converted to DXF (Drawing Interchange Format) files. In addition, the laser system also came with a software called SmartCarve4, which converts the DXF files into a series of commands for adjusting the power and translation speed of the laser according to our design requirements.

Three crucial parameters affecting the profiles of the ablated channels, namely the among of defocus (measured by taking the actual distance between the laser head and the top of sample) (k), laser power (pwr), and translation speed of the laser head (v), were optimized during the fabrication process. Briefly, k was fixed at 6 mm, pwr was set between 4 - 48 W, and v was in the range of 0 mm/s to 100 mm/s. A series of scribing trials on Parafilm® and PMMA were performed accordingly and at least five independent ablation processes with identical settings were performed for the data presented in this study.

Thermal fusion bonding

After laser ablation, PMMA slides and Parafilm[®] films cut to the desired dimensions were aligned and placed on a hotplate (MS-280-H, Hangzhou Jingfei Instrument Technology Co., LTD) together with a rectangular stone block for adding a calibrated static pressure at the top. The bonding temperature was varied between 25–100°C for different samples. The 5 kg stone block was capable of introducing a bonding pressure between 8.3 and 33.3 kPa. For uniform pressure distribution, a 5mm thick PMMA spacer slide was placed between the block and the sample stack (Figure 1). The pressure was applied for 20 minutes at the molding temperature and then maintained until the temperature dropped to room temperature, which takes around 40 minutes.

Characterization by Microscopy

The geometry of ablated microstructures was observed by an optical microscope (Olympus BH2-UMA) equipped with a digital camera (PROMICRA). Trypan blue dye (Yik Fung Scientific Co.) was injected into the microchannels for better visualization. Channel widths were measured across the micro channel as shown in Fig. 3. For the chips requiring a hydrophobic treatment, a water-repellent agent (47100, Aquapel, Pittsburgh, PA, USA) was first injected into the microchannels, followed by baking at 50°C on a hotplate until the Aquapel had dried out. The PLT fabricated chips, both with and without hydrophobic treatment, were sliced utilizing the same CO₂ laser system to obtain a cross-sectional structure. The cross-sectional structure of microchannels was examined by scanning electron microscopy (SEM) (FEI QUANTA 400F). Prior to SEM imaging, the samples were sputter-coated with gold. Imaging and monitoring of bacteria culture were carried out with a fluorescence microscope (Nikon).

Mechanical Characterization

Mechanical characterization was conducted using a tensile tester (QT/1L, QTest[™], MTS Systems Corporation). Tensile testing experiments were conducted to investigate the mechanical properties of Parafilm[®], which relates to its feasibility to be used as a flexible membrane for the fabrication of actuators such as microvalve and micropumps. Specimens were held in grips with a gauge length of 90 mm and stretched at a constant strain rate of 1% per minute.

Parafilm[®] with different gauge widths (10 mm, 15 mm, 20 mm) and an identical width of 25 mm in the grip section were prepared for tensile testing. Both untreated (Parafilm[®] as received) and heating treated Parafilm[®] (placed on the hotplate at 50 °C and 85 °C for 20 minutes, respectively) were tested to investigate the effect of heating treatment on the mechanical properties of Parafilm[®]. To investigate the combined effect of heating treatment and pressure on the mechanical properties of Parafilm[®], 50 °C treated Parafilm[®] with a static pressure of 0 or 0.4 kPa were tested.

The shear force-to-failure of the PLT fabricated chips was examined through tensile loading at a different direction (shear mode settings) using the same equipment. Specimens were fabricated utilizing different substrate materials (PMMA, PVC, Glass) and two thermal fusion bonding temperatures (50°C and 85°C), respectively. In each specimen, a Parafilm[®] slide, which has a size of three possible areas (10mm×10mm, 20mm×10mm, 40mm×10mm), is sandwiched between two mismatched substrates having the same area and material. A gauge length of 10 mm with a constant crosshead speed of 1mm/min was utilized to press one of the substrates, and the shear force-to-failure was recorded as the maximum force that the bonding structure could resist.

All testing experiments were carried out at room temperature. Each experiment was repeated for five times.

Microvalve and Micropump

A custom-made valve controller system, consisting of an ELVEFLOW microfluidic flow controller (OB1 MK3+ Microfluidic Flow Controller, ELVEFLOW) and ELVEFLOW Smart Interface software, was used for actuating the microvalves and micropumps fabricated with the PLT method. The pressurized nitrogen gas from outlets of the controller were injected into the PLT fabricated chips containing functional elements. This system is capable of controlling the actuation of PLT fabricated microvalves using compressed nitrogen gas at a maximum pressure of 200 kPa.

Cell culture in bioreactor

Frozen stock of recombinant Escherichia coli (E. coli) expressing green fluorescent protein (GFP) was resuspended in Lysogeny broth (25 g/L, Sigma) supplemented with 50 µg/mL of kanamycin (Sigma), transferred onto an agar plate, cultivated at 37°C for 2 days. Populations were established by inoculating 5 mL of liquid medium with a single-isolated colony and cultivated at 37°C for another day. The cultivated bacteria were diluted to 1×10^6 cells/mL for the subsequent experiments. Prior to the loading, the bioreactor was sterilized by rinsing of 75% ethanol followed by deionized water, air dried and irradiation with ultraviolet light for 30 minutes. 100 µL of bacteria suspension was manually injected into each chip. The inlet and outlet were then blocked to prevent evaporation and contamination during the 7-days culture at 37°C.

Results

Effects of laser power and laser scanning speed

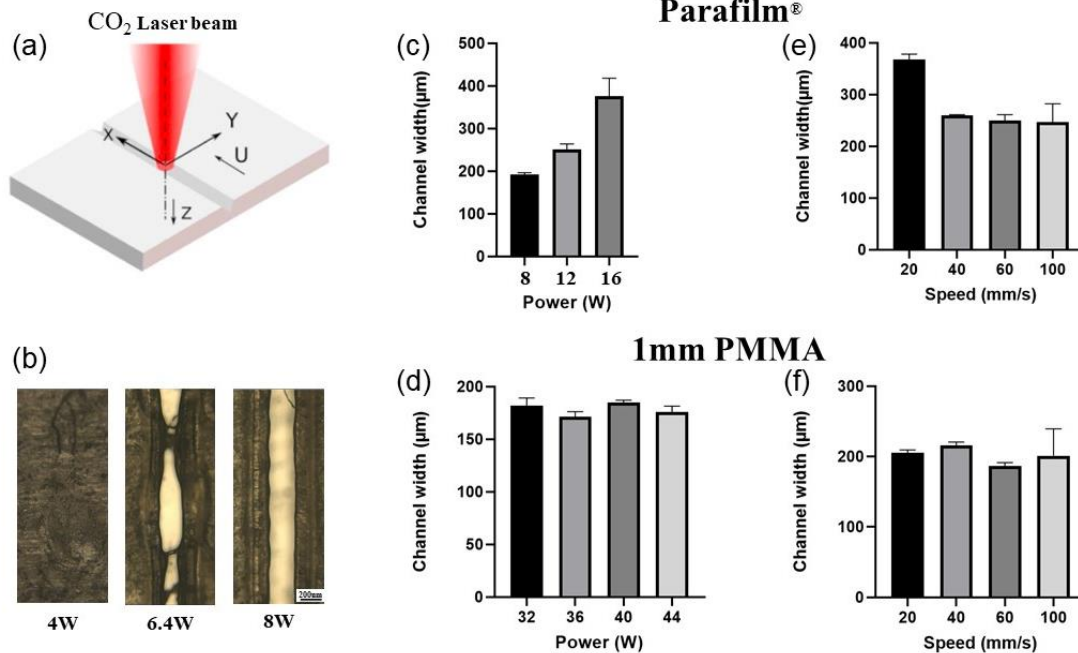


Fig.2. Illustration of laser ablation process (a) and effects of laser power and laser speed on the geometry of laser-plotted pattern (b)-(f). For each data point in figures (c)-(f), the experiment was carried out 5 times and average value was plotted with $k = 6.0$ mm. (c) Laser power vs. channel width for Parafilm[®] with $v = 60.0$ mm/s; (d) Laser power vs. channel width for 1mm PMMA with $v = 60.0$ mm/s; (e) Laser head moving speed vs. channel width for Parafilm[®] with $pwr = 10.0$ W; (f) Laser head moving speed vs. channel width for 1mm PMMA with $pwr = 36.0$ W.

The laser ablation process is shown as Fig.2(a). As shown in Fig.2(b), with the laser power increased from 4W to 8W, the patterns on the Parafilm[®] surface became consistent channels, from non-through scratches and discontinuous traces. As to achieve a continuous channel with smallest width and standard deviation, the laser power was set of 8W for the laser ablation process of Parafilm[®] as Fig.2(c) shows, maintaining a constant channel width of 249.1 ± 4.9 μm . Similarly, as is shown in Fig. 2(d), for the laser ablation process of 1mm PMMA substrate, the laser power was set of 36.0 W to achieve the smallest channel width, which is 171.4 ± 4.8 μm .

It was found that the laser head moving speed affects the channel width and the channel uniformity for the laser ablation process of Parafilm[®]. As is shown in Fig. 2(e), it was found that when the laser head moving speed was increased beyond 60 mm/s, the channel width was decreased from 367.73 ± 10.57 μm for 20 mm/s to 249.79 ± 11.22 μm for 60 mm/s. With the laser head moving speed increased from 60 mm/s to 100 mm/s, the channel width became 246.55 ± 35.67 μm , with a significant increase of standard deviation, indicating a decrease of channel uniformity. Similar results have been observed for the laser ablation process of PMMA substrates as Fig. 2(f) show. The smallest channel width of 186.74 ± 4.76 μm could be achieved with the laser head moving speed of 60 mm/s.

For the subsequent investigations, the laser power and speed were set at $k = 6.0$ mm, $pwr = 10.0$ W, $v = 60$ mm/s for Parafilm[®], and $k = 6.0$ mm, $pwr = 36.0$ W, $v = 60$ mm/s for 1mm PMMA substrate. Correspondingly, the optimized parameters for 2mm PMMA substrate are $k = 6.0$ mm, $pwr = 80.0$ W, $v = 60$ mm/s; for 2mm PVC substrate are $k = 6.0$ mm, $pwr = 80.0$ W, $v = 60$ mm/s for 2 times; for 2mm glass substrate are $k = 6.0$ mm, $pwr = 80.0$ W, $v = 10$ mm/s for 80 times (optimization process not shown here). All the chips, microvalves, micropumps, and bioreactors reported in this study were fabricated using this optimized laser ablation procedure.

Effects of bonding temperature and static pressure on Parafilm® deformation

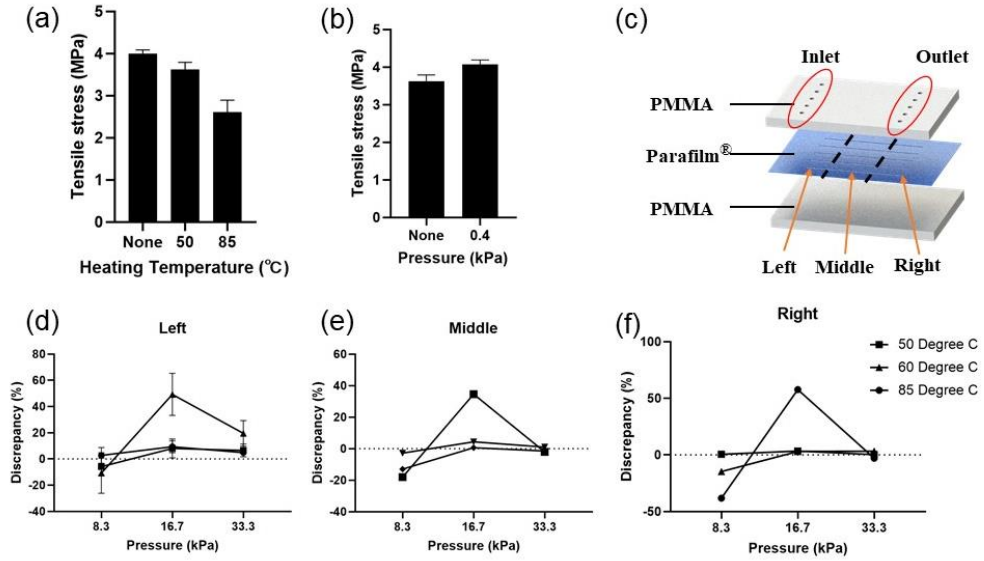


Fig. 3. Effects of temperature and pressure on Parafilm® mechanical properties and deformation of thermal bonding process. (a) Ultimate tensile stress of Parafilm® with thermal treatment. (b) Ultimate tensile stress of Parafilm® heated with 50°C heating treatment and pressure treatment. (c) Chip design for discrepancy tests. (d-f) Discrepancy (channel width deformation) of PLT fabricated chip with different heating temperatures.

Parafilm® with different gauge widths (10 mm, 15 mm, 20 mm) and an identical width of 25mm in the grip section and 9 mm gauge length were tested. For the heating-treated ones, specimens were put on the hotplate with different combinations of temperature (room temperature, 50°C, and 85°C) and pressure (0 and 0.4 kPa). The results of Parafilm® with a gauge width of 15 mm is shown as Fig. 3(a) and 3(b), and the results of 10 mm and 20 mm could be found in the supplementary information. As is shown in Fig. 3(a), the ultimate tensile stress decreased with increasing heating temperature. From Fig. 3(b), for the Parafilm® with 50°C heating treatment, an increase of 0.5 MPa of ultimate tensile stress was observed by adding 0.4 kPa pressure. Both untreated and treated Parafilm® had much higher ultimate tensile strengths than PDMS, which were often stated to be less than 1 MPa in the literature.²¹ Also, the ultimate tensile stress of untreated and treated Parafilm® specimens had significant difference ($P \leq 0.05$). Thus, the heating treatment and static pressure treatment affect the mechanical properties of the Parafilm® significantly.

In the process of thermal fusion bonding, the PLT chips was fabricated with a Parafilm® layer sandwiched between two PMMA layers as Fig. 3(c) shows. In this experiment study, the Parafilm® layer was designed to include 5 channels (width designed of 500 μm and length designed of 3 cm). Correspondingly, the top layer of 2 mm thick PMMA sheet has 5 inlets and 5 outlets at the two ends. The thermal fusion bonding was performed under the conditions with different combinations of temperature (25°C, 50°C, 60°C and 85°C) and pressure (8.3 kPa, 16.7kPa, 33.3 kPa) over a period of 20 minutes heating and 20 minutes cooling. After injecting trypan blue water into the chips, the channel width of Parafilm layer for each chip was measured and the discrepancy (channel width deformation) is shown from 3(d) to 3(f). The discrepancy between the design and the fabricated chip is characterized by calculating the changes of size as follows:

$$\Delta_{\text{width}} = [(W_{\text{before bonding}} - W_{\text{after bonding}}) / W_{\text{before bonding}}] \times 100\%$$

Where Δ_{width} defines the discrepancy(channel width deformation) of channel, $W_{\text{before bonding}}$ and $W_{\text{after bonding}}$ are the width of channel before and after thermal bonding process, respectively.

It was found that both the temperature and pressure of thermal fusion bonding affect the channel discrepancy and channel leakage. For the chips fabricated at 50°C and 60°C, increasing static pressure during thermal fusion bonding did not lead to any significant change in channel width. Obvious deformation of the channel (discrepancy of 49.26%) has been observed for the condition of 85°C and 33.3 kPa, with two channels at the two ends being blocked. It is interesting to note that a static pressure of 16.7 kPa resulted in the narrowest channel with among the three bonding pressures for the chips fabricated at 85°C.

As expected, without the assistance of heating (room temperature, 25°C), the adhesion force between Parafilm® and PMMA sheets is not strong enough to prevent leakage even at low pressure (put magnitude). After injecting Trypan Blue dye inside the chips fabricated at 25°C, obvious leakage was observed within 10 minutes (Supplementary Figure S3). Minimal leakage was observed for the chips fabricated at 50°C, 60°C and 85°C.

Overall, when Parafilm® works as a bonding agent, best results can be achieved with thermal fusion bonding temperature kept at 85°C; while for membrane microfluidic structures, the heat-assisted bonding process is carried out at 50°C. All chips, microvalves, micropumps, and bioreactors reported in this study were prepared using this optimized bonding procedure.

Mechanical strength of Parafilm® bonding

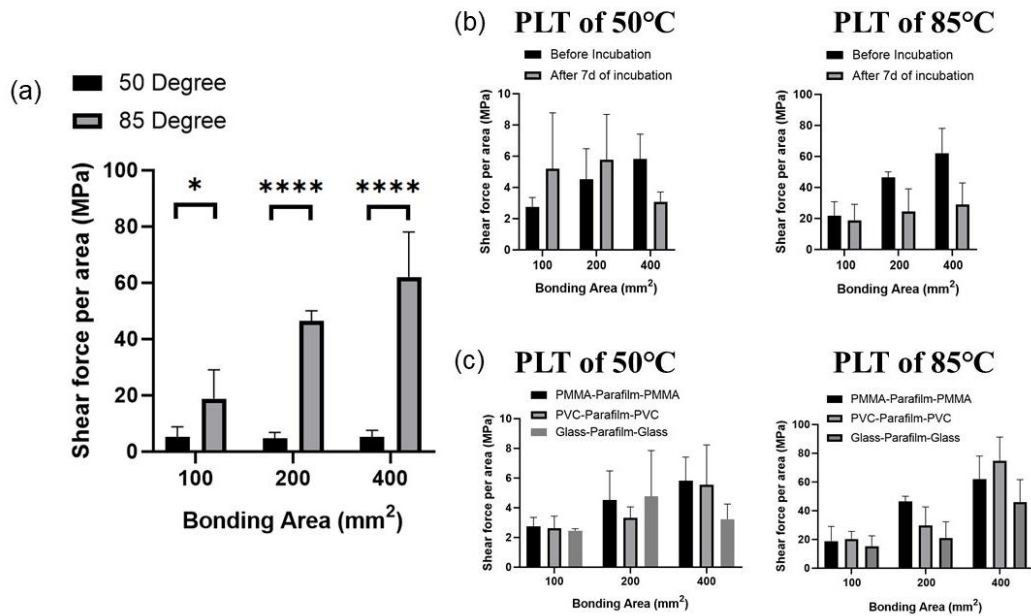


Fig. 4. Shear stress-to-failure for PLT biochip fabricated (a) with a thermal fusion temperature of 50°C and 85°C and bonding area of 10mm by 10mm, 10mm by 20mm, 10mm by 40mm, respectively. (b) PLT fabricated chip subjected for 7 days to 37.0 °C and 5% CO₂ atmosphere simulating cell culture conditions to those direct after bonding. (c) PLT fabricated chip with PMMA, PVC and glass substrates. **** refers to $P \leq 0.0001$ (extremely significant), *** refers to $P \leq 0.001$ (statistically highly significant), ** refers

to $P \leq 0.01$ (substantive significant), * refers to $P \leq 0.05$ (statistically significant) and ns refers to $P > 0.05$ (not significant).

The shear force-to-failure of PLT fabricated biochips was tested to evaluate the bonding strength as described in previous section. Experiments were repeated for different fabrication temperatures, different bonding areas and different substrates. As is shown in Fig. 4(a), for all three cases of different bonding areas (100 mm², 200 mm² and 400 mm²), all bonding strength values of 85°C are significantly greater than those of 50°C. Besides, the bonding strength is approximately positive correlated with the bonding area. In addition, here the ultimate shear stress of specimens fabricated at different temperatures had significant difference ($P \leq 0.05$), which as well shows a change in the mechanical properties of Parafilm® before and during thermal fusion bonding. Fig. 4(b) presents results of bonding strength studies for number additional substrate materials. Besides, the effects of cell culture environment are also studied as Fig. 4(c) shows. Additionally, Table S1 presents information on bonding strength and reversibility of bonding extracted from previous publications for comparison with our results.

The PLT bonding method has been developed to accommodate different substrate materials, here we utilized PVC and glass as Fig. 4(b) shows. The results support the conclusion that the PLT bonding strategy can be utilized for bonding PVC and glass substrates with a sealing strength comparable to that of PMMA, thus expanding the scope of application of PLT bonding method.

Results in Fig.4(c) show prolonged heating at 37.0 °C in 5% CO₂ also helped us evaluate the long-term mechanical stability of the chips. Between directly after bonding and after 7-days of incubation, evident decreases of the bonding strength to all bonding areas are observed for the samples fabricated at 85°C, with the decrease gets more obvious when bonding area increased from 100 to 400 mm² (20.9% for 100 mm², 45.9% for 200 mm², and 53.5% for 400 mm²). However, there is a slight increase was shown for the chips of 100 and 200 mm² fabricated at 50°C while a 26.6% decrease was shown for 400 mm² chips.

As shown in Table S1, the bonding strength of PLT bonding was lower than that of UV bonding adhesive bonding (16 MPa), but over 10 times higher than the spontaneous conformal contact that PDMS establishes with substrates and with itself (smaller than 0.2 MPa). Besides, the patterned functional Parafilm® layer in this PLT method solves the problem that UV bonding adhesives could not achieve patterning and applying a uniform thickness. Compared to PDMS bonding, the PLT method has the similar ability to seal various planar substrates, such as thermal plastics and glass, while at least 10 times faster.

Micropump and microvalve characterization fabricated using PLT

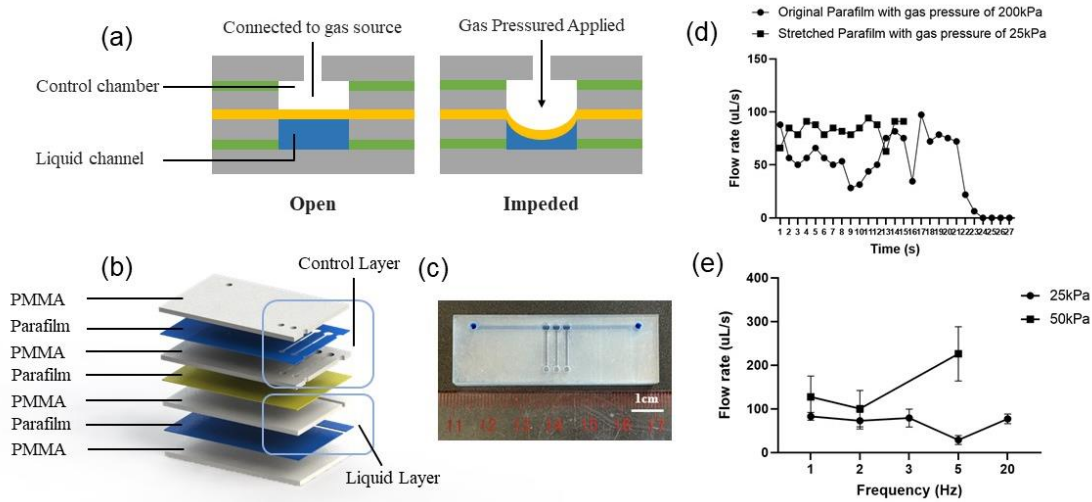


Fig. 5. Fabrication and characterization of the normally open microvalve and micropump. (a) Operation design of the microvalve. (b) 3D architecture of a fabricated chip with multiple microvalves. (c) Photograph and schematic showing a fabricated micropump. (d) Performance of the micropump fabricated with original Parafilm® and stretched Parafilm®. (e) Effect of actuation pressure and the frequency of actuation on pumping flow rate.

As shown in Fig.5(a), thermoplastic normally open microvalves were fabricated to investigate their functions in impeding aqueous liquid flow. Pressurized nitrogen gas was injected from the inlets to actuate the Parafilm® membranes located in the control membrane, leading to a deformation of the Parafilm® of control layer to impede the liquid flow in the fluid channel. A peristaltic micropump was developed by integration of three interconnected microvalves on a common liquid channel. As shown in Fig. 5(b) (c), the micropump is constructed of a control layer and a liquid layer. The Parafilm® of layer 2 and layer 6 (blue colored) work as a bonding media and the Parafilm® of layer 4 (yellow colored) has the functions of both bonding media and membrane structure. Especially, original Parafilm® without any treatment and Parafilm® been stretched manually have been utilized as layer 4 in fabrication process to fabricate micropump type1 and micropump type2, respectively. As shown in Fig. 5(d) (e), the effect of actuation gas pressure and the frequency of actuation on the pumping flow rate were studied, encompassing pressures of 25, 50, and 200 kPa and frequencies of 1, 2, 3, 5, and 20 Hz. The flow rate was measured by the volume of liquid filled in a tubing with a certain inner diameter during a specific period of time.

Initially, the bonding strength of the thermally bonded PMMA-Parafilm-PMMA layers constituting the microvalve architecture was tested. For both type1 and type2 chips, no burst failure was observed for liquid and gas pressures of up to 0.2 MPa, which were applied to the liquid channel and the control chambers, respectively. Subsequently, the deformation of the Parafilm® membrane upon applying nitrogen gas to the control chambers of type 1 chip was visualized as video 1 shows.

It has been observed that for type1 chip, the flow rate decreased from over 80 μL/s to 0 μL/s within 30s, which may be due to the fatigue failure of Parafilm®. While the pumping performance of type 2 chip is more stable and durable; the flow rate could be maintained at over 80 μL/s for more than 10 mins. For the type 2 chips, as the gas pressure was increased from 25 to 50 kPa, the flow rate obtained increased from 82.9 μL/s to 127.5 μL/s at the actuation frequency of 1 Hz.

SEM characterization of microchannels

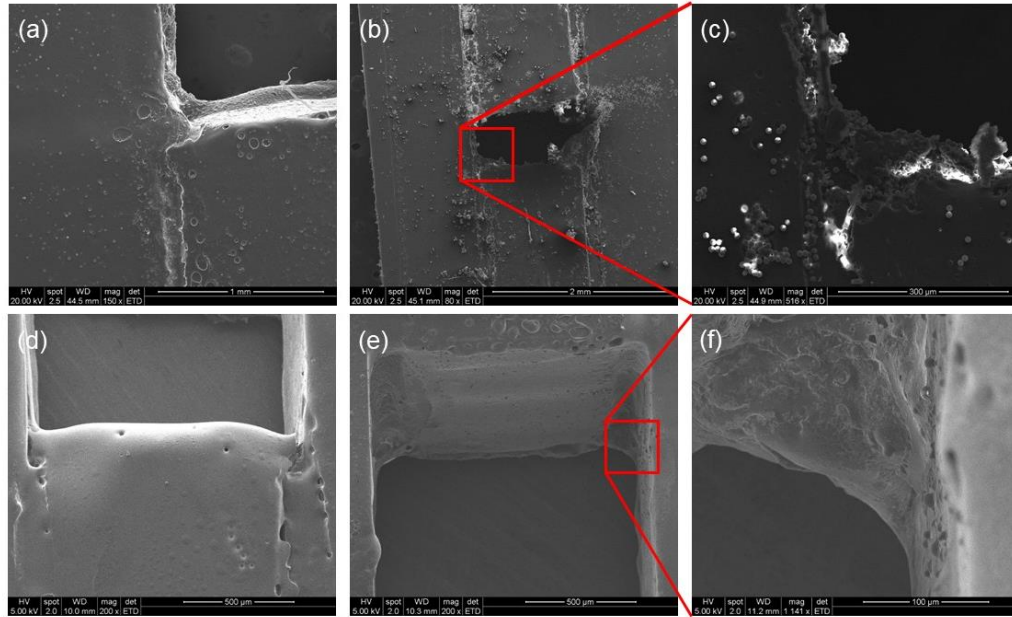


Fig. 6. SEM images of the cross sections of PLT fabricated microfluidic chips. (a) Microchannel without hydrophobic treatment, (b) after infusion of PS beads, (c) distribution of PS beads, (d) after hydrophobic treatment, (e) after infusion of PS beads and (f) distribution of PS beads. The dashed line on (a) and (d) indicates the interface between the PMMA substrate and Parafilm[®] of the channel.

The SEM images of the cross section of PLT fabricated chip were taken, indicating this PLT fabrication method can preserve the channel profile. Fig. 6(a) shows the cross section of PLT fabricated chip with a bonding temperature of 85°C and pressure of 33.3 kPa. Two lines can be observed between three layers in this figure, illustrating the interface between PMMA substrate and Parafilm[®]. To verify whether non-specific binding was presented, 10 μm polystyrene (PS) beads (Sigma-Aldrich Inc., Korea) were introduced into the PLT fabricated microchannels. From Fig. 6(b) and (c), a large number of PS beads were concentrated and forming obvious clusters at the interface of the microchannel regions, especially at the corner regions. This may come from the rough surface of melted Parafilm[®] and PMMA, which is caused by unequal heat distribution during the fabrication process.²² After the hydrophobic treatment of the microchannels, as Fig. 6(d) shows, the surface of microchannel has been more smooth, the interface between PMMA and Parafilm[®] became less clear. Fig. 6(e) and (f) show after infusion, more scattered distribution of PS beads at lower concentrations.

Bioreactor characterization

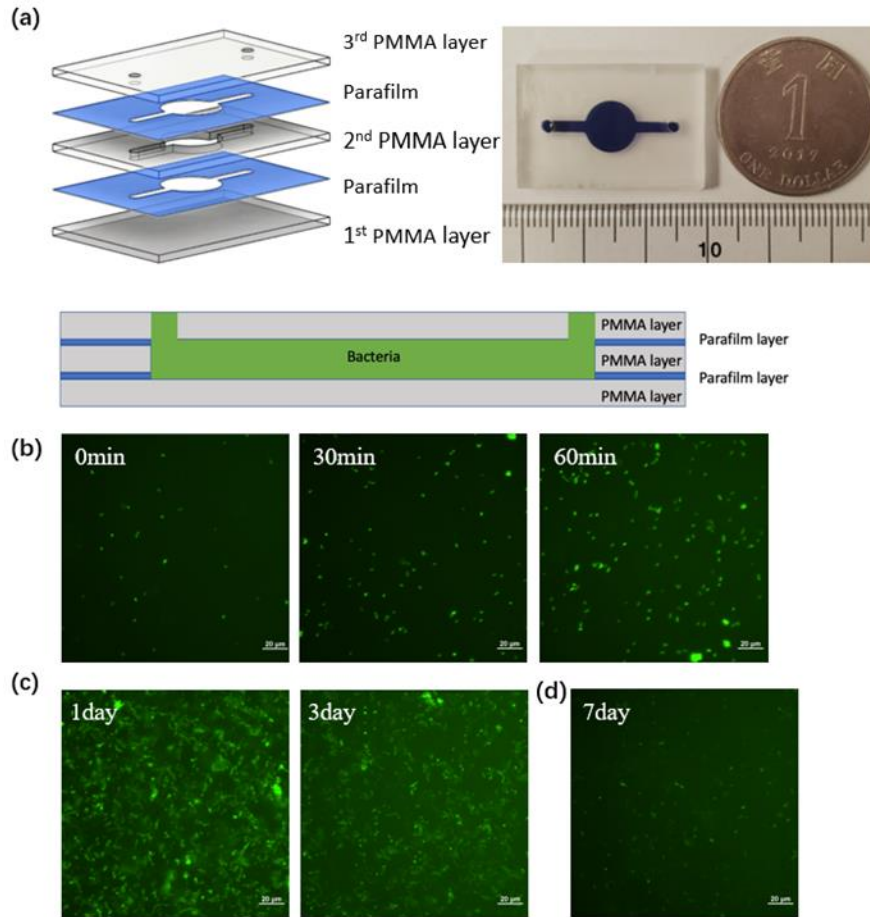


Fig. 7. Bacteria culture in PLT fabricated bioreactor. (a) Exploded view, cross-sectional view of the bioreactor, and the fabricated bioreactor. (b) Fluorescence images acquired at 0-min, 30-min, 60-min. (c) 1-day, 3-day post-cultivation in the bioreactor. (d) 7-day post-cultivation in the bioreactor (scale bar = 20 μm).

GFP-expressing *E. coli* were cultivated in the PLT fabricated bioreactor as shown in Fig. 7(a) to assess the biocompatibility. As observed from the fluorescent signal shown in Fig. 7(b) (c), the bacteria underwent proliferation and doubled roughly every 30 minutes, a similar doubling time typically observed in bulk liquid culture.²³ At 1-day and 3-day post-cultivation (Fig. 7 c), the growth of *E. coli* was observed arrested, presumably arriving the stationary phase or non-growth phase. When nutrients were mostly consumed at 7-day post-cultivation in a confined space, the green fluorescence was significantly decreased owing to the death of *E. coli*. (Fig. 7d), showing similar phenomena observed in typical liquid culture. Noted that minimal leakage was observed during the 7 days of bacterial culture.

Comparison of PLT method and other fabrication methods

	Soft lithography	Injection molding	PLT
Setup cost	~\$80k	>\$50k	<\$10k

Cost per print/materials	High	Low	Low
Turn-around time	~24h	3 weeks	<2h
3D capability	Layered 2D designs	Layered 2D designs	3D designs
Fluid automation	Routine	Difficult	Routine
Throughput	Low	Very high	High
Manufacturability	Poor	Poor	Good

a. Based on quotes from Black Hole Laboratories

b. Based on quotes for basic injection molding apparatus

Table 1. Comparison of PLT and conventional microfluidic chip fabrication methods

Conventional chip fabrication process, such as soft lithography, and injection molding is often very costly and time-consuming especially during the early stage of the research. Despite the high equipment price, high-standard labs and clean-room environments, requirements of tedious procedures, and poisonous chemicals (such as HF and SU8 solvent), the environmental factor is fundamentally in contrary to the original goals of microfluidics development: inexpensive, convenience, portability, environmentally friendly and disposability. The PLT, in contrary, provides a low-cost and time-saving solution to the fabrication of microfluidic chips as Table 1 shows. A typical several-day fabrication process is reduced nearly to 2 hours, with the fabrication materials easy to obtain.

Discussion

The creation of a novel and rapid prototyping approach for fabricating microfluidic chips out of Parafilm® and PMMA is demonstrated in this study. The laser plotting process as well as a high-strength thermal fusion bonding method were optimized to fabricate microfluidic chips. The Parafilm® 's high ultimate tensile stress was tested during mechanical characterization, allowing for the demonstration of high-performance actuators such as microvalves and micropumps. The bonding strengths of this method utilizing various substrate materials and after incubation treatment are also tested, revealed its possibility to be applied to diverse materials in different application scenarios. Gas-actuated microvalves were developed and operated without leakage. This PLT approach has also been applied to fabricate whole-thermoplastic bioreactors for cultivating GFP-expressing *E. coli* in a 7-day post-cultivation period.

As a convenient and time-saving prototyping method for fabricating microfluidic devices allowing large-scale manufacturing and packaging within a short cycle time, PLT agrees with the attributes in microfluidic fabrication: convenience, inexpensiveness, biocompatibility and disposability. The easy obtain-ability of fabrication materials as well as facilities (a single laser plotting machine and a hotplate are sufficient) make PLT a rapid and low-cost fabrication method in microfluidics applications. Besides, the diversified material selection provides possibility of enhancement in process compatibility.

References

1. Thompson, B. L. *et al.* A centrifugal microfluidic device with integrated gold leaf electrodes for the electrophoretic separation of DNA. *Lab Chip* **16**, 4569–4580 (2016).
2. Sackmann, E. K., Fulton, A. L. & Beebe, D. J. The present and future role of microfluidics in biomedical research. *Nature* **507**, 181–189 (2014).

3. Duffy, D. C., McDonald, J. C., Schueller, O. J. A. & Whitesides, G. M. Rapid prototyping of microfluidic systems in poly(dimethylsiloxane). *Anal. Chem.* **70**, 4974–4984 (1998).
4. Zhao, X. M. Soft lithographic methods for nano-fabrication. *J. Mater. Chem.* **7**, 1069–1074 (1997).
5. Unger, M. A., Chou, H. P., Thorsen, T., Scherer, A. & Quake, S. R. Monolithic microfabricated valves and pumps by multilayer soft lithography. *Science (80-.)*. **288**, 113–116 (2000).
6. McDonald, J. C. & Whitesides, G. M. Poly(dimethylsiloxane) as a material for fabricating microfluidic devices. *Acc. Chem. Res.* **35**, 491–499 (2002).
7. Lee, J. N., Park, C. & Whitesides, G. M. Solvent Compatibility of Poly(dimethylsiloxane)-Based Microfluidic Devices. *Anal. Chem.* **75**, 6544–6554 (2003).
8. Sollier, E., Murray, C., Maoddi, P. & Di Carlo, D. Rapid prototyping polymers for microfluidic devices and high pressure injections. *Lab Chip* **11**, 3752–3765 (2011).
9. Rajendrani Mukhopadhyay. When PDMS isn't the best. *Anal. Chem.* **79**, 3248–3253 (2007).
10. Weigl, B., Domingo, G., LaBarre, P. & Gerlach, J. Towards non- and minimally instrumented, microfluidics-based diagnostic devices. *Lab Chip* **8**, 1999–2014 (2008).
11. Ma, J. *et al.* A simple photolithography method for microfluidic device fabrication using sunlight as UV source. *Microfluid. Nanofluidics* **9**, 1247–1252 (2010).
12. Lu, R., Shi, W., Jiang, L., Qin, J. & Lin, B. Rapid prototyping of paper-based microfluidics with wax for low-cost, portable bioassay. *Electrophoresis* **30**, 1497–1500 (2009).
13. Shaegh, S. A. M. *et al.* Rapid prototyping of whole-thermoplastic microfluidics with built-in microvalves using laser ablation and thermal fusion bonding. *Sensors Actuators, B Chem.* **255**, 100–109 (2018).
14. Gong, X. *et al.* Wax-bonding 3D microfluidic chips. *Lab Chip* **10**, 2622–2627 (2010).
15. Wang, L. *et al.* Prototyping chips in minutes: Direct Laser Plotting (DLP) of functional microfluidic structures. *Sensors Actuators, B Chem.* **168**, 214–222 (2012).
16. Hong, T. F. *et al.* Rapid prototyping of PMMA microfluidic chips utilizing a CO2 laser. *Microfluid. Nanofluidics* **9**, 1125–1133 (2010).
17. Matellan, C. & Del Río Hernández, A. E. Cost-effective rapid prototyping and assembly of poly(methyl methacrylate) microfluidic devices. *Sci. Rep.* **8**, 1–13 (2018).
18. Lu, Y., Shi, Z., Yu, L. & Li, C. M. Fast prototyping of a customized microfluidic device in a non-clean-room setting by cutting and laminating Parafilm®. *RSC Adv.* **6**, 85468–85472 (2016).
19. Fu, J. J. *et al.* Cutting and Bonding Parafilm® to Fast Prototyping Flexible Hanging Drop Chips for 3D Spheroid Cultures. *Cell. Mol. Bioeng.* (2020). doi:10.1007/s12195-020-00660-x
20. Yu, L. & Shi, Z. Z. Microfluidic paper-based analytical devices fabricated by low-cost photolithography and embossing of Parafilm®. *Lab Chip* **15**, 1642–1645 (2015).
21. Johnston, I. D., McCluskey, D. K., Tan, C. K. L. & Tracey, M. C. Mechanical characterization of bulk Sylgard 184 for microfluidics and microengineering. *J. Micromechanics Microengineering* **24**, (2014).

22. Prakash, S. & Kumar, S. Experimental investigations and analytical modeling of multi-pass CO₂ laser processing on PMMA. *Precis. Eng.* **49**, 220–234 (2017).
23. Elbing, K. L. & Brent, R. Recipes and Tools for Culture of Escherichia coli. *Curr. Protoc. Mol. Biol.* **125**, 1–19 (2019).

Acknowledgements

The authors are grateful to the funding support from the Hong Kong Research Grants Council (project reference: GRF14204621, GRF14207920, GRF14207419, GRF14203919, N_CUHK407/16), and from the Innovation and Technology Commission (project reference: GHX-004-18SZ).

The authors would like to acknowledge Mr. Guangyao Cheng (Department of Biomedical Engineering, The Chinese University of Hong Kong) for his support of building the custom-made valve controller system. The authors would also like to acknowledge the technical support provided by the Department of Physics for providing the access to SEM imaging facility. And thanks for Dr. Ryan Xie, Dr. Md Habibur Rahman, Ms. Shiyue Liu, Mr. Jianxin Yang, Mr. Kelvin Pong, Ms. Wanyi Zhang and Mr. Shaodi Zhu (Department of Biomedical Engineering, The Chinese University of Hong Kong) for their advice as well as continuous encouragement.

Author information

Affiliations

The Chinese University of Hong Kong

Yuanyuan Wei, Tianle Wang, Yi-Ping Ho, Ho-Pui Ho

Shenzhen Institutes of Advanced Technology

Yuye Wang

Author contributions

Yuanyuan Wei conceived and conducted the experiments and the paper writing of laser ablation, thermal fusion bonding, characterization by microscopy, mechanical characterization, as well as microvalve and micropump. Tianle Wang conceived and conducted the experiment and the paper writing of cell culture in bioreactor. Yuye Wang participated in the project conceiving. Yi-Ping Ho and Ho-Pui Ho conceived the project and supervised the research. All authors reviewed the manuscript.

Corresponding author

Correspondence to Yi-Ping Ho and Ho-Pui Ho.

Ethics declarations

Competing interests

The authors declare no competing financial interests.

Additional information

Publisher's note Springer Nature remains neutral with regard to jurisdictional claims in published maps and institutional affiliations.

Electronic supplementary material

Supplementary Material

Supplementary Video 1

Supplementary Video 2

Rights and permissions

Open Access This article is licensed under a Creative Commons Attribution 4.0 International License, which permits use, sharing, adaptation, distribution and reproduction in any medium or format, as long as you give appropriate credit to the original author(s) and the source, provide a link to the Creative Commons license, and indicate if changes were made. The images or other third party material in this article are included in the article's Creative Commons license, unless indicated otherwise in a credit line to the material. If material is not included in the article's Creative Commons license and your intended use is not permitted by statutory regulation or exceeds the permitted use, you will need to obtain permission directly from the copyright holder. To view a copy of this license, visit <http://creativecommons.org/licenses/by/4.0/>.

Supplementary Files

This is a list of supplementary files associated with this preprint. Click to download.

- [SUPPLE1.pdf](#)
- [SupplymentaryVideo1.mp4](#)
- [SupplymentaryVideo2.mp4](#)